# SYNTHESIS AND CHARACTERIZATION OF POLYMER COMPOSITE FERROELECTRIC MATERIALS

---

A Dissertation Submitted in partial fulfilment
FOR THE DEGREE OF MASTER OF SCIENCE IN PHYSICS
Under Academic Autonomy

## NATIONAL INSTITUTE OF TECHNOLOGY, ROURKELA

**By**

## ANIL KUMAR MOHAPATRA

Under the Supervision of

**Prof. S. Panigrahi**



DEPARTMENT OF PHYSICS
NATIONAL INSTITUTE OF TECHNOLOGY
ROURKELA – 769008

**May 2011**

# NATIONAL INSTITUTE OF TECHNOLOGY
## ROURKELA

## <u>CERTIFICATE</u>

This is to certify that the thesis entitled, **"Synthesis and characterization of polymer composite  ferroelectric materials***"* submitted by Mr. Anil Kumar Mohapatra in partial fulfillments for the requirements for the award of Master of Science Degree in Physics Department at National Institute of Technology, Rourkela is an authentic work carried out by him under my supervision and guidance.

To the best of my knowledge, the matter embodied in the project has not been submitted to any other University/ Institute for the award of any Degree or Diploma.

<br>

Rourkela

Date:13.05.2011

Prof. S. Panigrahi
Dept. of Physics
National Institute of Technology
Rourkela-769008

# ACKNOWLEDGEMENTS

I humbly prostrate myself before the Almighty for his grace and abundant blessings which enabled me to complete this work successfully.

It gives me great pleasure to express my deep sense of gratitude and regards to my supervisor **Prof. S Panigrahi** for initiating me to work in the field of "Synthesis and characterization of polymer composite ferroelectric materials" under his guidance. His great interest, encouragement and guidance had made my work fruitful.

I extend my sincere thanks to Mr. V Senthil for his invaluable suggestions and help throughout my dissertation work.

I am extremely thankful to Prof. S Jena, Head, Department of Physics and the faculty members of Physics department for providing all kinds of possible help and advice during the course of this work.

I record my sincere thanks to Department of Ceramic Engineering, for the help in taking XRD, Department of Metallurgical and Material Science for extending all facilities to carry out the SEM.

I would also like to thank all the research scholars and my class mates of our Physics department for their inspiration and help.

Lastly my hearty thanks to my parents and my brother for their blessings, inspiration and moral support.

Date: 13.05.2011                                          **Anil Kumar Mohapatra**

*Dedicated to my parents*

*whose love has contributed*

*so much to my strength and faith*

# CONTENTS

# ABSTRACT

Polymer-ceramic composites combine superior properties of both polymer and ceramics which result in far better performance than those of the constituent materials. Polymers are flexible, easy to fabricate and superior in dielectric break down strength. On the other hand, ferroelectric ceramics possess high dielectric permittivity but with poor mechanical properties and lower dielectric breakdown strength. By integrating high dielectric permittivity ceramic powder with superior dielectric strength of the polymer, one can develop a composite with high dielectric permittivity and high breakdown strength. This type of composites has high capability of energy storage and can be used in capacitors and energy storage device.

The $Ba_{1-x}Sr_xZr_{0.1}T_{0.9}O_3$ Powders were prepared by conventional solid-state reaction route, Ba replaced by Sr in A site of $BaZr_{0.1}Ti_{0.9}O_3$ ceramic in different value of x(i.e x=0.0,0.1,0.2,0.3). Preliminary X-ray Structural analysis for $Ba_{1-x}Sr_xZr_{0.1}T_{0.9}O_3$ powders suggested the formation of single-phase compound in tetragonal crystal system. Then the polymer composite ferroelectric material is prepared by using polyvinyl alcohol (PVA) as a polymer matrix.

The polymer composite XRD pattern as same as ferroelectric ceramic patterns, it may be the ceramic powder dominating over the polymer. This may be due to the increase of amorphous nature of PVA with the addition of ferroelectric ceramic. The SEM micrograph shows that the BSZT particle distribution is homogenous with no porous in the PVA matrix. Detailed studies of dielectric and impedance properties of the material in a wide range of frequency (100Hz-1MHz) and temperatures (30-120$^0$C) shows that these properties are strongly temperature and frequency dependent.

## CHAPTER-1

### 1. Introduction

Ceramic materials and single crystals showing ferroelectric behaviour are being used in many applications in electronics and optics. Ferroelectric can be utilized in various devices such as high-permittivity dielectrics, pyroelectric sensors, piezoelectric devices, electro-optic devices and PTC components.

### 1.1 Ferroelectricity

Ferroelectricity is the phenomenon which refers to the state of spontaneous polarization, i.e., polarization of the material in the absence of an electric field. It is thus analogous to ferromagnetism which represents the state of spontaneous magnetization of the material. The crystals exhibiting ferroelectricity are called the ferroelectric crystals. In such crystals, the centres of positive and negative charges do not coinside with each other even in the absence of electric field, thus producing a non-zero value of the dipole moment. The variation of polarization with electric field is not linear for such crystals but forms a closed loop called the hysteresis loop is shown in (fig.1).
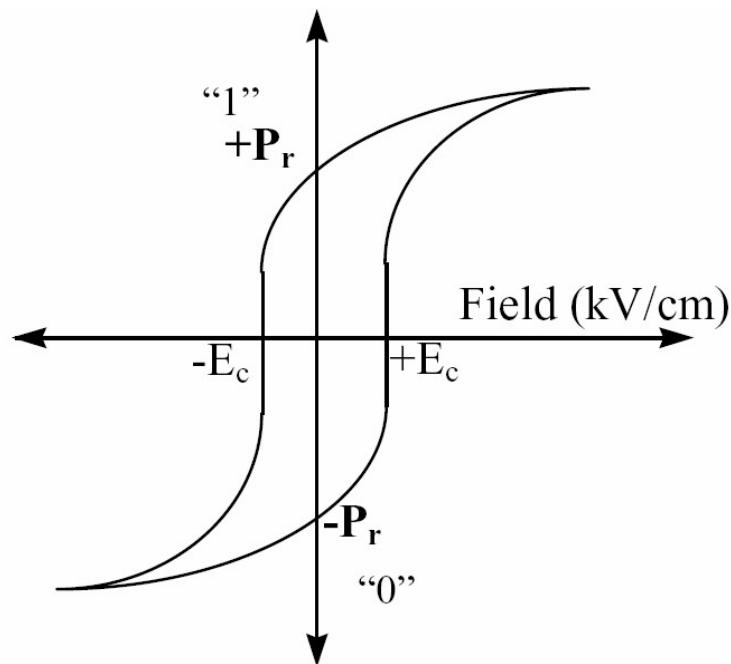


**Fig.1** Polarization vs. Electric Field (P-E) hysteresis loop for a typical ferroelectric crystal

As the electric field strength is increased, the domains start to align in the positive direction giving rise to a rapid increase in the polarization. At very high field levels, the polarization reaches a saturation value ($P_s$). The polarization does not fall to zero when the external field is removed. At zero external fields, some of the domains remain aligned in the positive direction; hence the crystal will show a remnant polarization ($P_r$). The crystal cannot be completely depolarized until a field of magnitude is applied in the negative direction. The external field needed to reduce the polarization to zero is called the coercive field strength ($E_c$). If the field is increased to a more negative value, the direction of polarization flips and hence a hysteresis loop is obtained. The value of the spontaneous polarization ($P_s$) is obtained by extrapolating the curve onto the polarization axes.

All ferroelectric materials have a transition temperature called the Curie point ($T_c$). At a temperature $T > T_c$ the crystal does not exhibit ferroelectricity, while for $T < T_c$ it is ferroelectric. On decreasing the temperature through the Curie point, a ferroelectric crystal undergoes a phase transition from a non-ferroelectric phase to a ferroelectric phase. If there are more than one ferroelectric phases, the temperature at which the crystal transforms from one ferroelectric phase to another is called the transition temperature. The temperature dependence of the dielectric constant above the Curie point ($T > T_c$) in ferroelectric crystals is governed by the Curie-Weiss law $= C/(T-T_0)$, where C and $T_O$ are the Curie-Weiss constant and Curie-Weiss temperature, respectively.



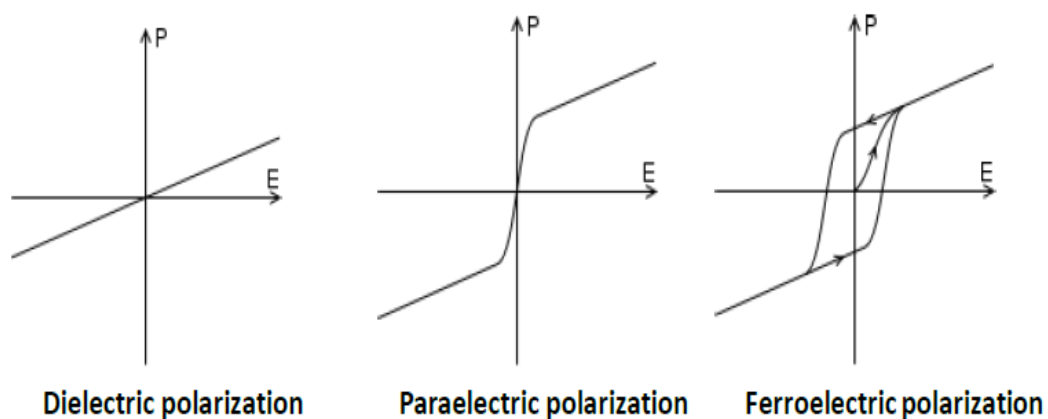Dielectric polarization     Paraelectric polarization     Ferroelectric polarization

**Fig.2** Polarization Vs. Electric field (P-E) loop for different materials

Most materials are polarized linearly with external electric field; nonlinearities are insignificant. This is called dielectric polarization (Fig.2). Some materials, known as

paraelectric materials, demonstrate a more pronounced nonlinear polarization. In addition to being nonlinear, ferroelectric materials demonstrate a spontaneous (zero field) polarization. Such materials are generally called pyroelectrics. The distinguishing feature of ferroelectrics is that the direction of the spontaneous polarization can be reversed by an applied electric field, yielding a hysteresis loop. Typically, materials demonstrate ferroelectricity only below a certain phase transition temperature, called the Curie temperature, $T_c$, and are paraelectric above this temperature.

## 1.2 Classification of ferroelectric materials

The ferroelectric crystals may be classified into two main groups:

### (i)The order-disorder group

In the order-disorder class of ferroelectrics, the ferroelectric transition is associated with indivisual ordering of ions. These are the crystals which contain hydrogen bonds and in which the motion of protons is related to the ferroelectric properties.

**Examples:** Potassium dihydrogen phosphate ($KH_2PO_4$), Rubidium hydrogen phosphate ($RbH_2PO_4$) etc.

### (ii)The displacive group:

The displacive group of ferroelectrics is the one in which the ferroelectric transition is associated with the displacement of a whole sub lattice of ions of one type relative to a sublattice of another type. The crystals of this class exhibit structures which are closely related to the Perovskite and ilmenite structures.

**Examples:** $BaTiO_3$, $KNbO_3$, $LiTaO_3$

## 1.3 Basis for the Ferroelectricity in Crystals

Solid matter can be described as:

**a. Amorphous:** The atoms are arranged in a random way similar to the disorder we find in a liquid. Glasses are amorphous materials.

**b. Crystalline:** The atoms are arranged in a regular pattern, and there is as smallest volume element that by repetition in three dimensions describes the crystal. This smallest volume element is called a unit cell. The dimension of the unit cell is described by three axes: a, b, c and the angles between them $\alpha$, $\beta$, $\gamma$.
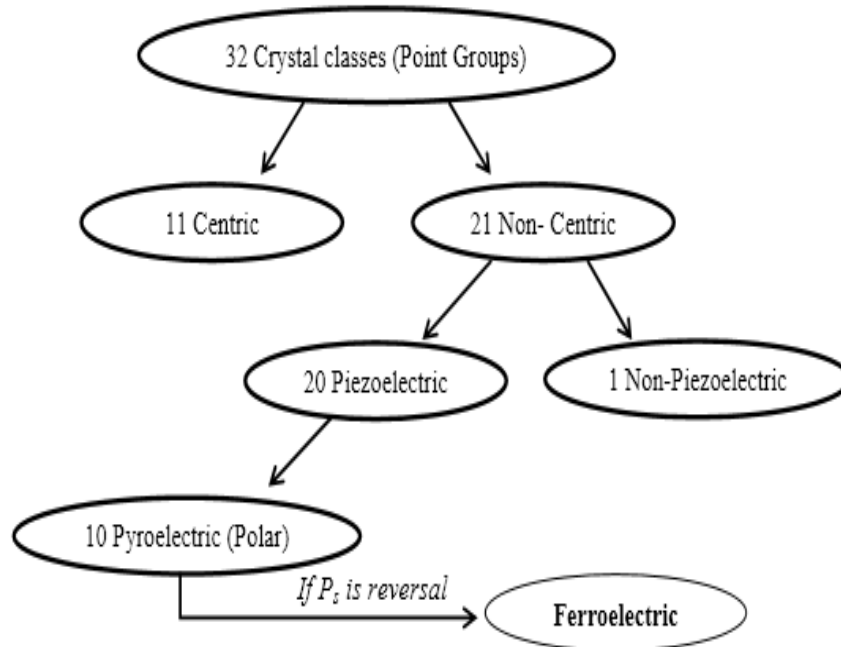


**Fig.3** A classification scheme for the 32 crystallographic point groups

Crystal can be divided into 32 groups. Of the 32 possible crystal classes (i.e. point groups), 11 are Centro symmetric and thus cannot exhibit polar properties. The remaining 21 lack a center of symmetry and thus can possess one or more polar axes. Among these, 20 classes are piezoelectric, the one exception being cubic class (Figure-3). Piezoelectric crystals have the property that the application of mechanical stress induces polarization, and conversely, the application of an electric field produces mechanical deformation. Of the 20 piezoelectric classes, 10 have a unique polar axis and thus are spontaneously polarized, i.e. polarized in the absence of an electric field. Crystals belonging to these 10 classes are called pyroelectric. However, because the polarization is a function of temperature, it is often possible to observe the spontaneous moment in these crystals by changing the temperature, hence the name pyroelectrics. Ferroelectric crystals belong to the pyroelectric family, but they also exhibit the additional property that the direction of the spontaneous polarization can be reversed by the application of an electric field.

## 1.4    Perovskite Crystal Structure

A perovskite structure is any material with the same type of crystal structure as calcium titanium oxide ($CaTiO_3$), Barium titanate (BT), Lead titanate ($PbTiO_3$), Lead Zirconate Titanate (PZT), Lead Lanthanum Zirconate Titanate (PLZT), and Potassium Niobate ($KNbO_3$) are known as the perovskite structure. Its simplest structure is cubic, which is the high temperature form of many mixed oxides of the $ABO_3$ type, where 'A' and 'B' are two cations of very different sizes, and X is an anion that bonds to both. Perovskite is the mineral name of Calcium Titanate ($CaTiO_3$) .The $ABO_3$ structure is shown in Figure 4.
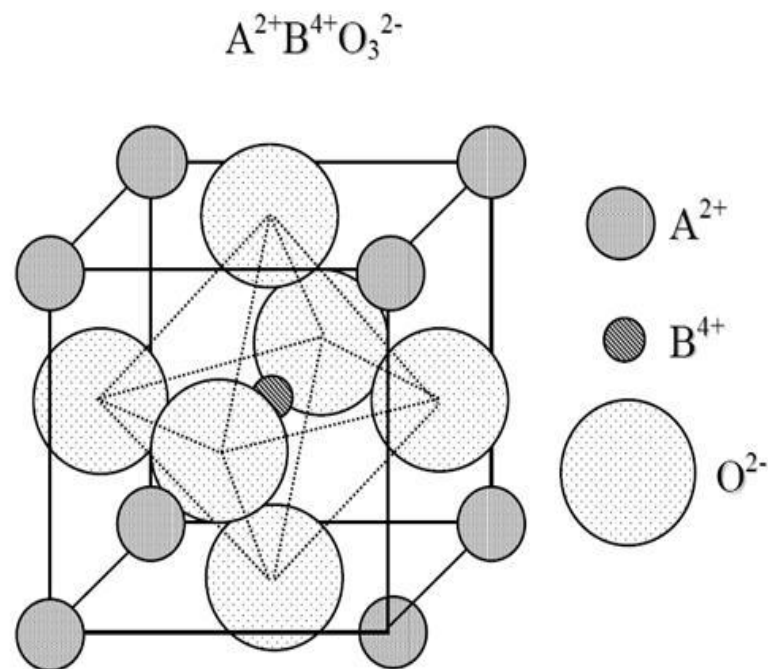
$$A^{2+}B^{4+}O_3^{2-}$$



$A^{2+}$

$B^{4+}$

$O^{2-}$

**Fig. 4**   A cubic $ABO_3$, perovskite type unit cell

## 1.5    Dielectrics and Insulators

The word dielectric is derived from the prefix dia, originally from Greek, which means "through" or "across"; thus, the dielectric is referred to as a material that permits the passage of the electric field or electric flux, but not particles. The dielectric is generally considered a non-conducting or an insulating material that can be polarized by an applied electric field. When a dielectric is placed in an electric field, electric charges do not flow through the material, as in a conductor, but only slightly shift from their

average equilibrium positions causing dielectric polarization. Because of dielectric polarization, positive charges are displaced toward the field and negative charges shift in the opposite direction. This creates an internal electric field which reduces the overall field within the dielectric itself.

An insulator, also called a dielectric, is a material that resists the flow of electric charge. In insulating materials valence electrons are tightly bonded to their atoms. These materials are used in electrical equipment as insulators or insulation. Their function is to support or separate electrical conductors without allowing current through themselves. The study of dielectric properties is concerned with the storage and dissipation of electric and magnetic energy in materials. It is important to explain various phenomena in electronics, optics, and solid-state physics.

## 1.6    Polymer composite ferroelectric materials

Fabrication of composite materials means to combine two or more different materials having different properties to obtain the desirable material properties that often cannot be obtained in single-phase materials. Now a day's polymer composite also received considerable attention as compared to ferroelectric ceramics in view of their technological importance in devices such as sensors, actuators, transducers etc. A material derived from polymer and ceramic phases is identified as a polymer-ceramic composite in this thesis.

Ferroelectric ceramics possessing very high dielectric constants are brittle and suffer from poor mechanical strength. On the other hand, polymers having low dielectric constants in the range of 2-5 traditionally used in low leakage capacitor are flexible, easy to process and possess high dielectric strength. New polymer-ceramics composites have high dielectric constant, and high dielectric breakdown strength to achieve high volume effiency and energy storage density for applications of capacitors and electric energy storage devices could be fabricated by combining the merits of polymers and ceramic. In order to achieve such an objective, high dielectric constant ferroelectric ceramics such as $BaTiO_3$ (BT), Pb (Zr, Ti) O3 (PZT) and PMNPT have been used as fillers in polymers. These composite materials possess superior physical properties such as enhanced mechanical strength and improved electric compliance.

Among the ferroelectric, Barium titanate ($BaTiO_3$) has been much studied for its numerous scientific and industrial applications, such as in dielectric capacitors, transducer and tunable phase shifter. The structure of $BaTiO_3$ is shown in fig.5.
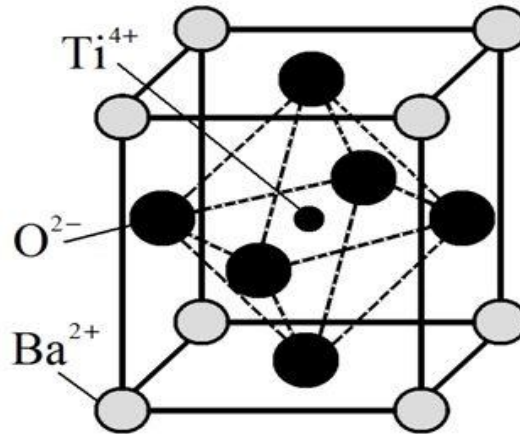


**Fig.5**    Structure of cubic $BaTiO_3$

However, $BaTiO_3$ has its own limitations in terms of the tenability of the dielectric constant, and also having limited utility in electromechanical transducers used under high hydrostatic condition because of low hydrostatic piezoelectric coefficient, high permittivity and high density. The $BaTiO_3$ powders have been used as filler and studied to explore the possibility of obtaining high dielectric constant composites for potential capacitor applications.

In this thesis Poly vinyl alcohol (PVA) was used as matrix material because of its better aqueous solubility, high tensile strength and flexibility. It has also odorless and nontoxic, resistant to oil, grease and solvent, which make it more suitable for making electronic components.

## 1.7 Thesis Objective

- To synthesis the ferroelectric material $(Ba_{1-x}Sr_xZr_{0.1}Ti_{0.9}O_3)$ by solid state reaction route.

- To synthesis the polymer composite of as synthesised ferroelectric material with Poly vinyl alcohol (PVA) by volume percentage.

- To characterize the synthesized polymer composite ferroelectric material by XRD for phase formation, SEM for surface morphology and electrical study for dielectric and impedance spectroscopy.

# CHAPTER-2

## EXPERIMENTAL TECHNIQUE

In this chapter the details of synthesis of the ceramic ferroelectric $(Ba_{1-x}Sr_xZr_{0.1}Ti_{0.9}O_3)$ powder, polymer composite ferroelectric material and the experimental technique employed to characterize the specimen are briefly discussed.

## 2.1.    Synthesis of ceramics $(Ba_{1-x}Sr_xZr_{0.1}Ti_{0.9}O_3)$
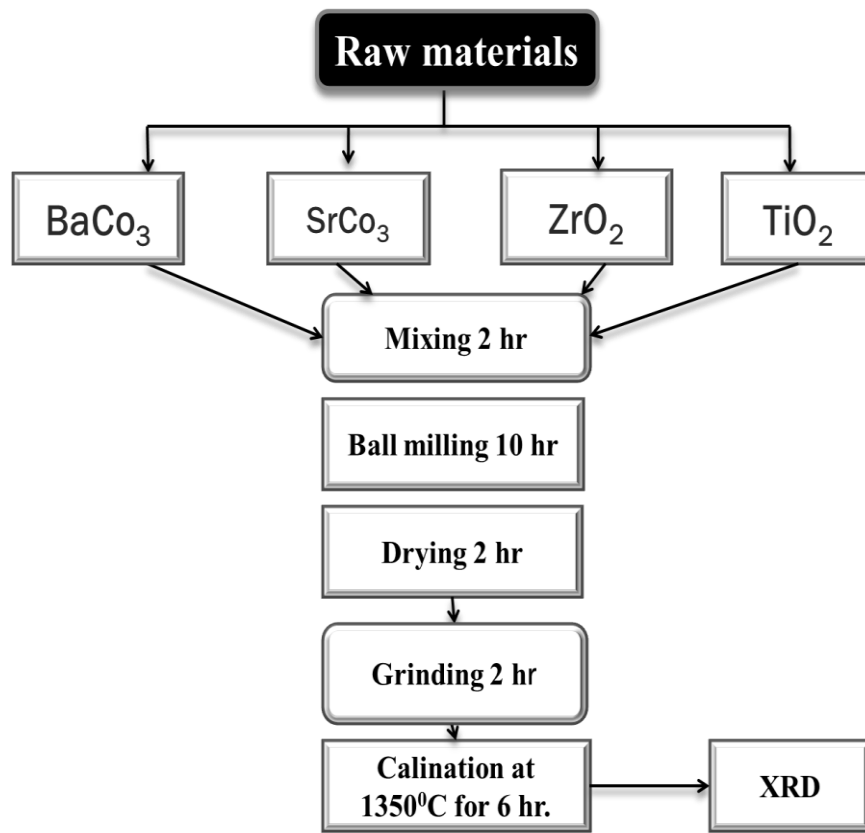


**Fig.6** Flow chart for synthesis of Sr doped ceramic $(Ba_{1-x}Sr_xZr_{0.1}Ti_{0.9}O_3)$

The Sr doped $(Ba_{1-x}Sr_xZr_{0.1}T_{0.9}iO_3)$ ceramic were prepare by solid state reaction method by taking high purity raw materials such as (i) Barium Carbonate $(BaCO_3)$, (ii)Strontium carbonate$(SrCo_3)$,(iii)Zirconium dioxide $(ZrO_2)$ and (iv) Titanium dioxide $(TiO_2)$ . For the combination of these four raw materials $(Ba_{1-x}Sr_xZr_{0.1}Ti_{0.9}O_3)$ ceramic compound were formed, where x is the Sr concentration in $(Ba_{1-x}Sr_xZr_{0.1}Ti_{0.9}O_3)$ ceramic compound (i.e., x = 0, 0.1, 0.2, 0.3). The constituents of the required specimen are taken in a stoichiometric ratio. The mixing is accomplished using agate mortar and pestle. Then

the ceramics were ball-milled for 10hrs for proper mixing of the powders in acetone medium by using zirconia balls. Then the mixed powders were kept in programmable furnace at $1350^0$ C for 6hrs with intermediate mixing and grinding for the phase formation and removal of a volatile fraction.

The various steps in solid state reaction process are represented as a flow chart shown in Figure 6.

## 2.2. Synthesis of Polymer composite (PVA - $Ba_{1-x}Sr_xZr_{0.1}Ti_{0.9}O_3$)
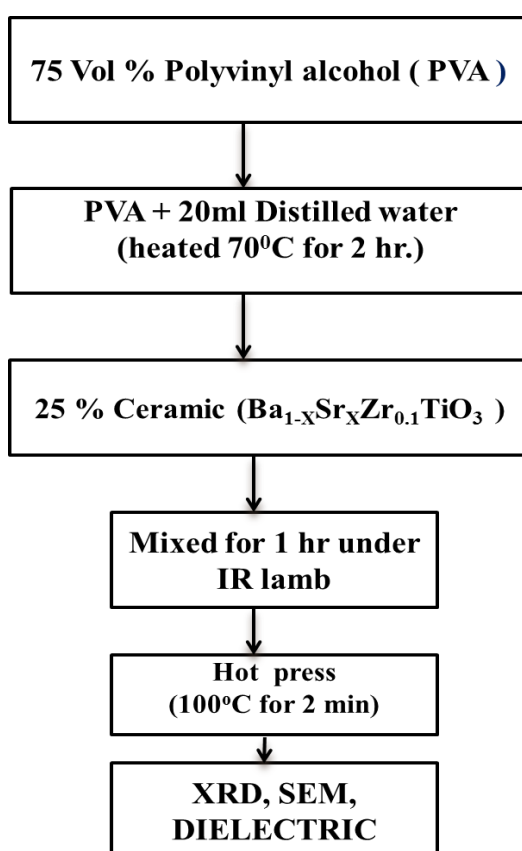
```
┌─────────────────────────────────────┐
│  75 Vol % Polyvinyl alcohol ( PVA )  │
└─────────────────────────────────────┘
                  │
                  ▼
┌─────────────────────────────────────┐
│      PVA + 20ml Distilled water       │
│       (heated 70⁰C for 2 hr.)         │
└─────────────────────────────────────┘
                  │
                  ▼
┌─────────────────────────────────────┐
│  25 % Ceramic (Ba₁₋ₓSrₓZr₀.₁TiO₃ )   │
└─────────────────────────────────────┘
                  │
                  ▼
        ┌────────────────────┐
        │  Mixed for 1 hr under │
        │       IR lamb        │
        └────────────────────┘
                  │
                  ▼
        ┌────────────────────┐
        │     Hot  press       │
        │  (100ºC for 2 min)   │
        └────────────────────┘
                  │
                  ▼
        ┌────────────────────┐
        │      XRD, SEM,       │
        │     DIELECTRIC       │
        └────────────────────┘
```

**Fig. 7.** Flow chart for Synthesis of PVA-($Ba_{1-x}Sr_xZr_{0.1}Ti_{0.9}O_3$)

For preparation of polymer composite (PVA-$Ba_{1-x}Sr_xZr_{0.1}Ti_{0.9}O_3$) in the ratio of vol%75/25, 0.96 gm. of PVA and 1.505 gm. of ceramic ($Ba_{1-x}Sr_xZr_{0.1}Ti_{0.9}O_3$) were taken. Then 0.96 gm. of PVA was added into 20 ml distilled water and stirred constantly at $70^0$C for 2 h by using a magnetic stirrer. Then the 1.505grm of ceramic ($Ba_{1-x}Sr_xZr_{0.1}Ti_{0.9}O_3$) was added with PVA suspension by using an agate mortar for 1 hr under IR lamp. Finally for the fabrication of (PVA/BaSrZrTiO$_3$) composite was hot-pressed at $100^o$C for 2 min

with the pressure of 5tons. Then the prepared PVA-($Ba_{1-x}Sr_xZr_{0.1}Ti_{0.9}O_3$) composite was kept for XRD, SEM and electrical study. For electrical study, silver paste has used for the electrode of the both sides of the samples. The similar procedure have been used for PVA100 vol% and PVA 50 vol% for the composition of $Ba_{1-x}Sr_xZr_{0.1}Ti_{0.9}O_3$ (x=0) only.

The various steps in the preparation of polymer composites are represented as a flow chart as shown in Figure-7.

## 2.3. Synthesis method

The following synthesizing tools are used to prepare the ceramic materials and polymer composite.

### 2.3.1. Ball Mill

Ball mill is an efficient tool for grinding many materials into fine powder. The Ball Mill is used to grind many kinds of mine and other materials, or to select the mine, widely used in building material, chemical industry, etc. Ball mills rotate around a horizontal axis, partially filled with the material to be ground plus the grinding medium. Different materials are used as media, including ceramic balls, flint pebbles and stainless steel balls. An internal cascading effect reduces the material to a fine powder. The difference in speeds between the balls and grinding jars produces an interaction between frictional and impact forces, which releases high dynamic energies. The interplay between these forces produces the high and very effective degree of size reduction of the planetary ball mill.

### 2.3.2. Calcination

Calcination is a thermal treatment process applied to ores and other solid materials in order to bring about a thermal decomposition, phase transition, or removal of a volatile fraction. The calcination process normally takes place at temperatures below the melting point of the product materials. Calcination is to be distinguished from roasting, in which more complex gas-solid reactions take place between the furnace atmosphere and the solids.

### 2.3.3. Hot press

It is not always possible to obtain a low-porosity body by 'pressure less sintering, i.e. by sintering at atmospheric pressure. More commonly it may prove difficult to combine the complete elimination of porosity with the maintenance of small crystal size. These problems can usually by overcome by hot-pressing, i.e. sintering under pressure between punches in a die. The pressure now provides the major part of the driving force eliminating porosity and the temperature can be kept at a level at which crystal growth is minimized.

### 2.4.   Characterization methods

The following characterizing tools are used to study the structural, morphological and electrical study of the ceramics.

### 2.4.1   X-Ray diffraction study

X-rays are electromagnetic radiations. Its wavelength is smaller than that of visible light. X-ray tube is used to generate these rays. In this tube a high voltage is applied across the electrodes. Because of this high voltage the electrons in the tube get accelerated and hit a metal target (anode). X-rays are produced due to this. X-rays tubes containing copper targets are commonly used for structural characterization of materials.

X-ray diffractometer works on the principle of Bragg's law. A crystal consists of Parallel atomic planes. If a beam of X-ray falls on such a plane then according to Bragg's law the diffracted beam will have a maximum intensity if

$$2d \sin\theta = n\lambda$$

Where d is spacing between atomic planes, $\lambda$ is wavelength of X-ray used, $\theta$ is angle of diffraction and n = 1, 2, 3……..

The X-ray diffractometer gives a plot of intensity of diffracted beam as a function of the angle $2\theta$. The x-ray diffraction technique is a versatile method to determine the different phases, crystal structure, lattice defects, lattice strain and the crystallite size (in case of Nano-particles) with a great accuracy.

### 2.4.2 Scanning Electron Microscope (SEM)

In SEM when a beam of highly energetic electrons strikes the sample, the secondary electrons, x-rays and back-scattered electrons are ejected from the sample. These electrons are then collected by the detector and convert into signal that displays on a screen. As the samples are non-conducting, a thin layer of platinum is coated using a sputter coater. Generally SEM only provides information about the surface of the specimen and not the internal contents.

### 2.4.3 Dielectric Measurement

In this work Salotron gain/phase impedance analyser were used to measure the dielectric measurement. The electrode samples were used to make the measurements. The Salotron gain/phase impedance analyser was interfaced with the computer and the data was collected as a function of frequencies at different temperatures.

### 2.4.4 Impedance spectroscopy

Impedance spectroscopy measures the dielectric properties of a medium as a function of frequency. It is based on the interaction of an external field with the electric dipole moment of the sample, often expressed by permittivity. This technique measures the impedance of a system over a range of frequencies, and therefore the frequency response of the system, including the energy storage and dissipation properties, is revealed. Impedance is the opposition to the flow of alternating current (AC) in a complex system.

AC measurements are often made with a Wheatstone bridge type of apparatus in which the resistance R and capacitance C of the sample are measured and balanced against variable resistors and capacitors. The impedance $|Z|$ and the phase difference ($\theta$) between the voltage and current are measured as a function of frequency for the given sample and the technique is called impedance spectroscopy. Analysis of the data is carried out by plotting the imaginary part of the impedance $Z''=|Z|\cos\theta$ against the real part $Z'=|Z|\sin\theta$ on a complex plane called the impedance plot.

# CHAPTER-4

# RESULTS AND DISCUSSION

## 4.1 XRD Analysis

The $Ba_{1-x}Sr_xZr_{0.1}Ti_{0.9}O_3$ ceramics were prepared by solid state reaction route. The XRD pattern of the Sr doped $BaZr_{0.1}Ti_{0.9}O_3$ ceramic powder calcined at $1350^0C/6$ h is shown in figure 8 and 9. According to JCPDS no.05-0626, all the peaks in the patterns are matching and its showing purely tetragonal single phase crystal related to tetragonal $BaTiO_3$. The single phase crystals of the $Ba_{1-x}Sr_xZr_{0.9}Ti_{0.1}O_3$ ceramics are tetragonal symmetry in the space group P4mm. While increasing the concentration of Sr in $Ba_{1-x}Sr_xZr_{0.1}Ti_{0.9}O_3$, the composition x=0.3 matched with JCPDS no.44-0093 having space group P4mm and showing tetragonal structure of $BaTiO_3$. As the $Sr^{2+}$ content is increased the peaks in the pattern shift towards right (increase in the 2θ position), which shows the shift in 2θ position clearly (fig. 10). This shift is obvious because of the substitution of smaller ionic size $Sr^{2+}$ in place of larger ionic size $Ba^{2+}$. The c/a ratio gives the value of more than 1 and it confirms the tetragonal phases. Peak position, FWHM, volume of the unit cell and lattice parameters are tabulated in the Table.1.

In order to investigate the influence of ferroelectric on polymer matrix, X-ray diffraction studies were performed for pure PVA and BSZT based ferroelectric ceramic. Fig 11 shows the x-ray diffraction pattern of pure 100 vol% of pure PVA and 50 vol % of PVA with ceramic. In figure 11, a broad peak around $20.3^o$ was observed in pure PVA films, and this can be attributed to the semi crystalline behavior of the polymer corresponding to the orthorhombic lattice structure. It is evident from the figure that there is a relative decrease in the intensity of this peak with the increase of dopant concentration. This may be due to the increase of amorphous nature of PVA with the addition of ferroelectric ceramic. Figure 12 indicates the 75 vol % of PVA and 25 vol% of ceramic having composition x=0.0, 0.1, 0.2.

The polymer composite XRD pattern as same as ferroelectric ceramic patterns, it may be the ceramic powder dominating over the polymer. This may be due to the increase of amorphous nature of PVA with the addition of ferroelectric ceramic.
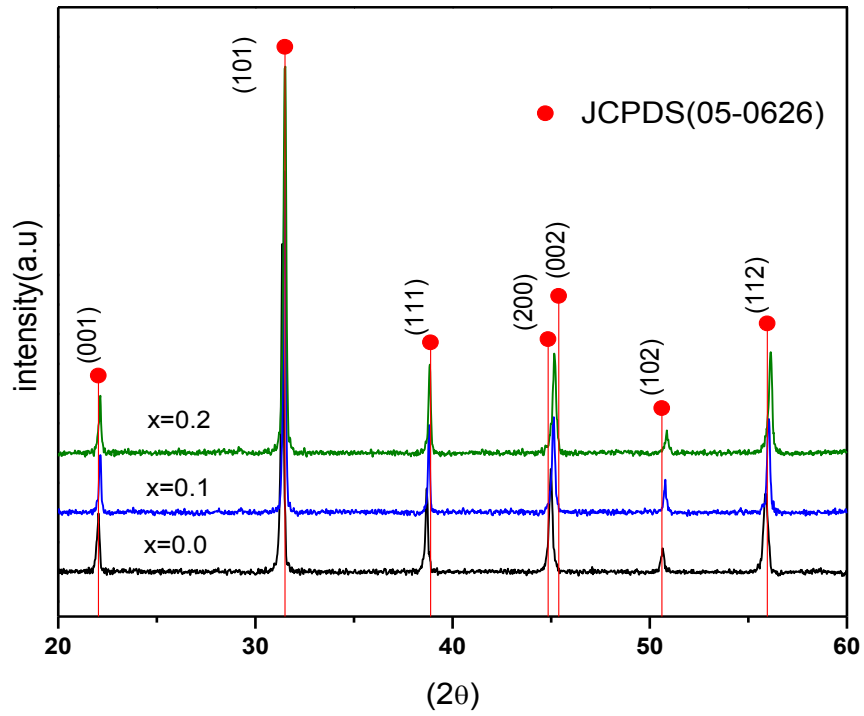
**Fig. 8.** X-ray diffraction patterns for the calcined ceramic (Ba$_{1-x}$Sr$_x$Zr$_{0.1}$Ti$_{0.9}$O$_3$) powder at 1350$^0$C/6 h
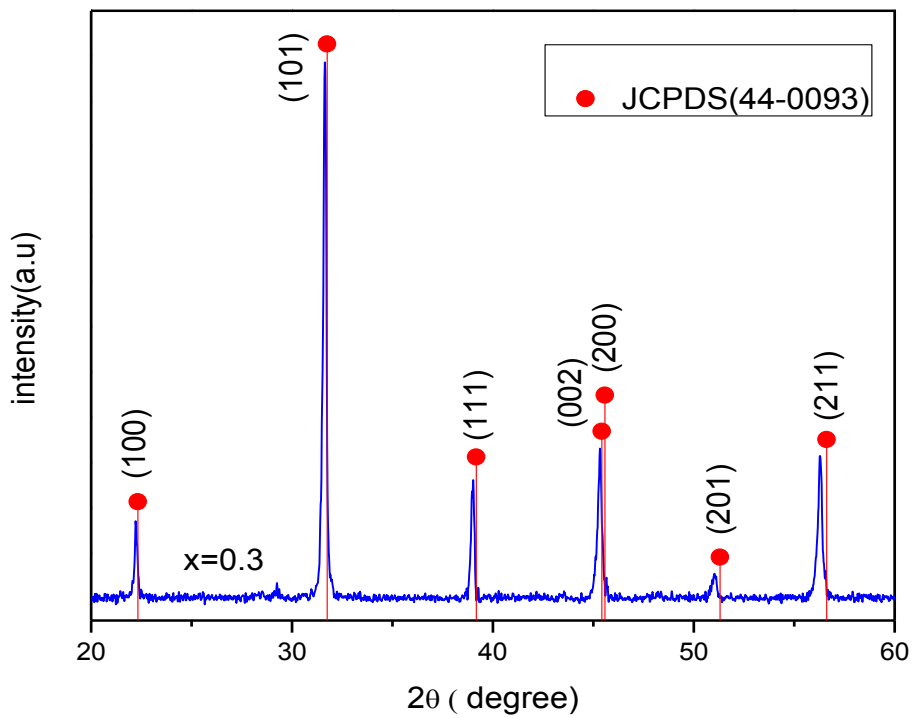


**Fig. 9.** X-ray diffraction patterns for the calcined ceramic (Ba$_{1-x}$Sr$_x$Zr$_{0.1}$Ti$_{0.9}$O$_3$) powder at 1350$^0$C/6 h
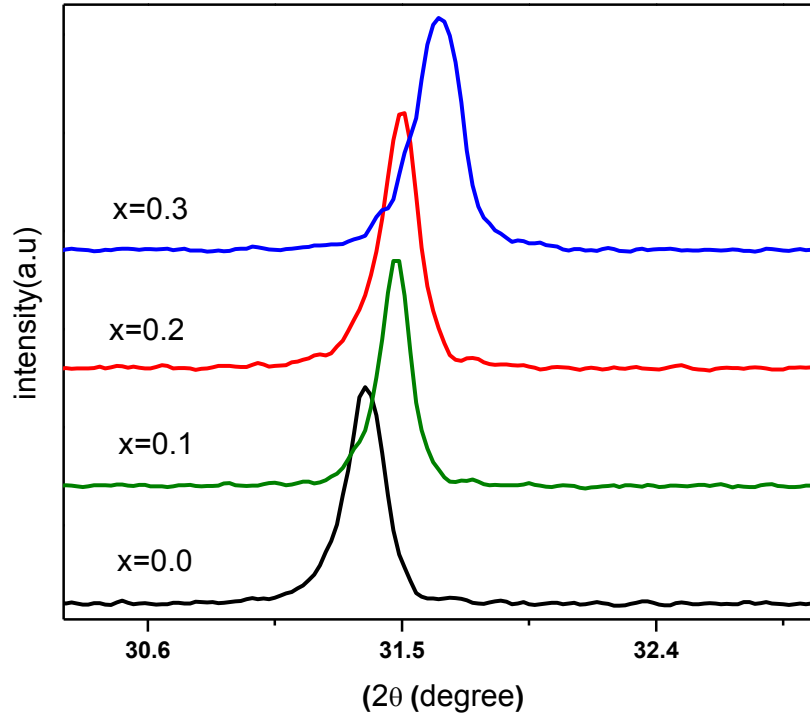
**Fig. 10.** Shifting of peaks for the calcined ceramic $(Ba_{1-x}Sr_xZr_{0.1}Ti_{0.9}O_3)$ powder at $1350^0C/6$ h

**Table-1** Peak position, FWHM, lattice parameters for all composition of $Ba_{1-x}Sr_xZr_{0.1}Ti_{0.9}O_3$

| sample | Con(x) | 2 θ in degree | FWHM | a=b | C | Volume |
|--------|--------|---------------|--------|--------|--------|--------|
| 1 | 0.0 | 31.3789 | 0.1680 | 4.0263 | 4.0278 | 65.30 |
| 2 | 0.1 | 31.4845 | 0.1200 | 4.0155 | 4.0173 | 64.78 |
| 3 | 0.2 | 31.5060 | 0.1440 | 4.0091 | 4.0169 | 64.56 |
| 4 | 0.3 | 31.6728 | 0.1680 | 3.9917 | 4.0323 | 64.25 |

**~ 16 ~**
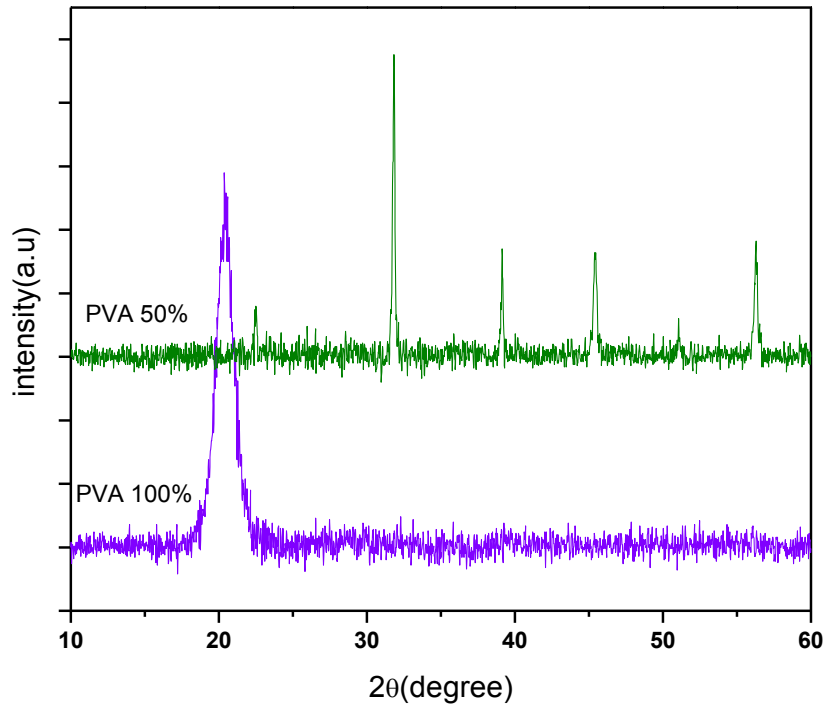
**Fig. 11.** X-ray diffraction patterns for hot pressed PVA100 vol % and ceramic (x=0.0) 50 vol % with PVA 50 vol %
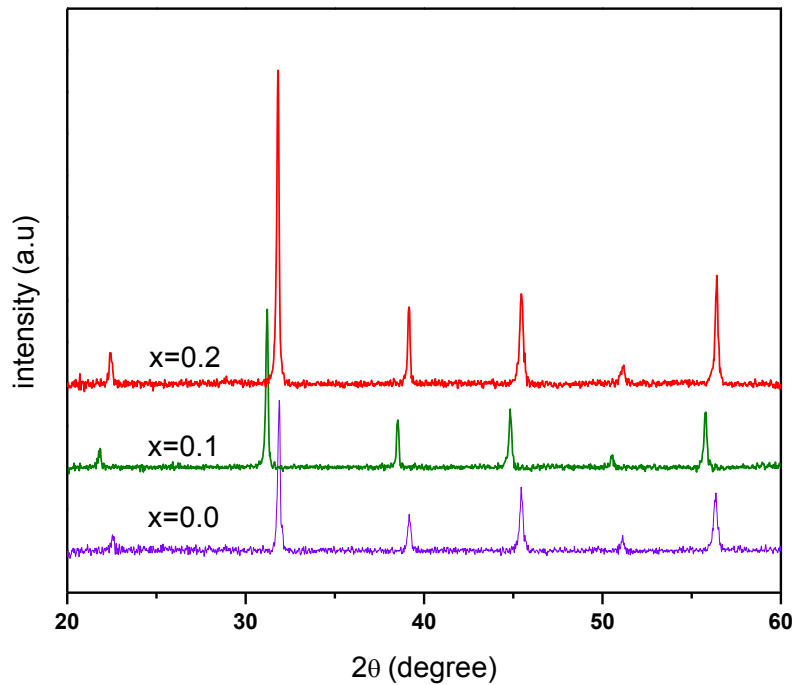


**Fig.12.** X-ray diffraction patterns of hot pressed polymer composite ceramic $(Ba_{1-x}Sr_xZr_{0.1}Ti_{0.9}O_3)$

## 4.2. SEM Analysis

Figure 13 shows the surface morphology of the hot-pressed 100 vol% of PVA and polymer composites containing various volume % of BSZT filler. It is seen that the BSZT particles are distributed homogenous with no porous in the PVA matrix .It also earlier reported that good dispersion of the ceramic filler can induce homogeneous packing leading to uniformity of properties and a higher dielectric constant. The morphology of the pure PVA and PVA/BZT 50:50, BSZT 75:25, studied by SEM technique, is a uniform type but with different degrees of roughness. In SEM micrographs of the composites, the light area corresponds to the ferroelectric ceramics and the dark region corresponds to the polymer matrix.
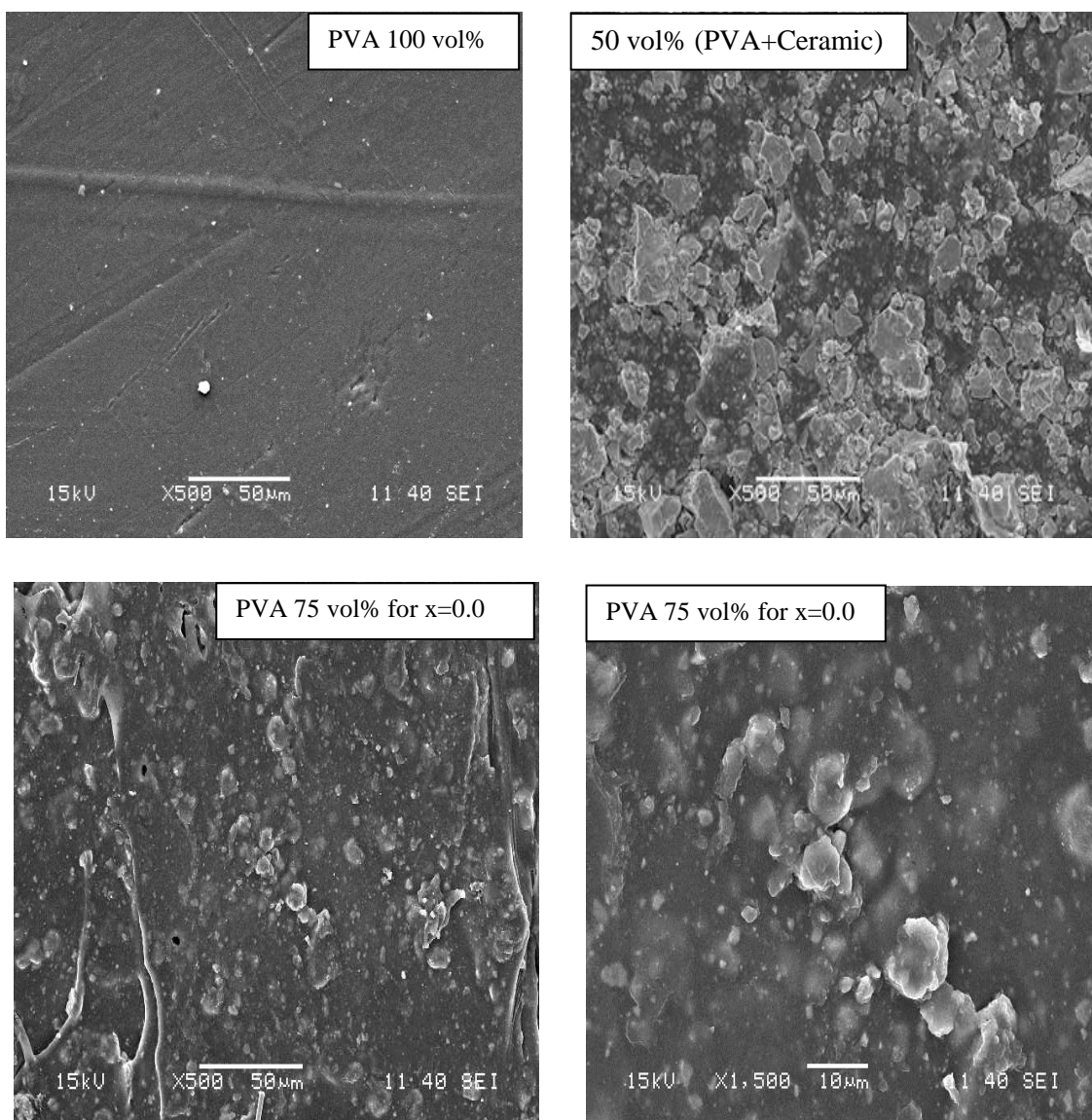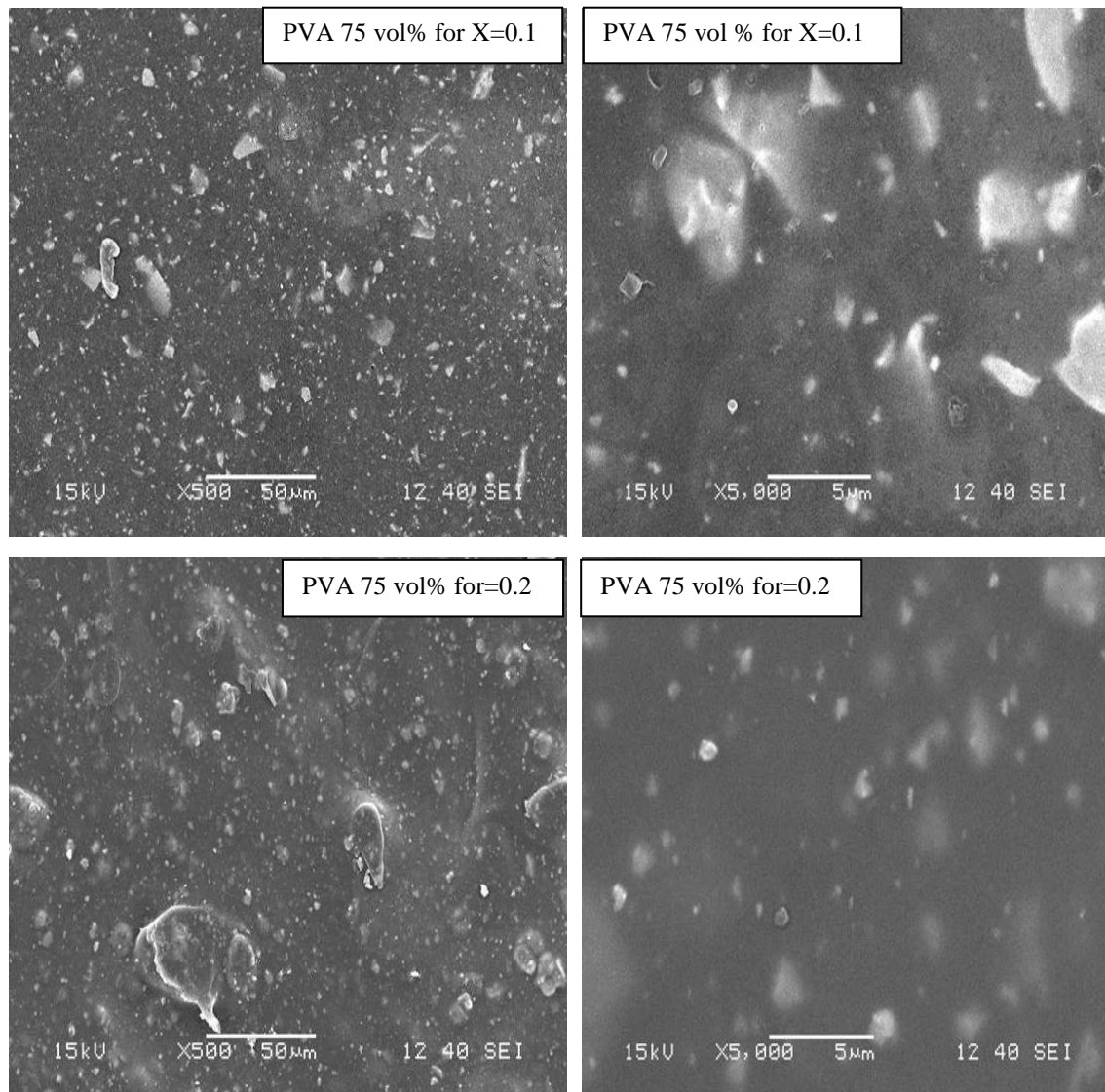
**Fig.13.** SEM micrographs of hot pressed polymer composite $Ba_{1-x}Sr_xZr_{0.1}Ti_{0.9}O_3$

## 4.3    Dielectric study

### 4.3.1    Temperature dependences of the dielectric study

The temperature dependences of the dielectric properties of PVA-BZT (75:25%) and PVA-BSZT (75:25%) at different frequency fields are illustrated in fig.14. As shown in Fig. 14, the dielectric constant gradually increased with increasing temperature. This observation is in other polymer/BaTiO$_3$ composites, where the $\varepsilon_r$ increased with temperature. Generally, the change of dielectric property in the composites includes three

competitive mechanisms: (a) the segmental mobility of polymer would improve with increasing temperature, which should facilitate the polarization of polar components and increase the dielectric constant consequently, (b) the thermal expansion of polymer could disrupt the chains of contact $BaTiO_3$ particles, which should reduce the dielectric constant and (c) the structure of $BaTiO_3$ particles could be changed with an increase in temperature (before Curie temperature), which could generate a modification on the dielectric response of the ceramic. According to the above literature, the dielectric constant is increased with increasing temperature in the polymer composite of PVA-BSZT.
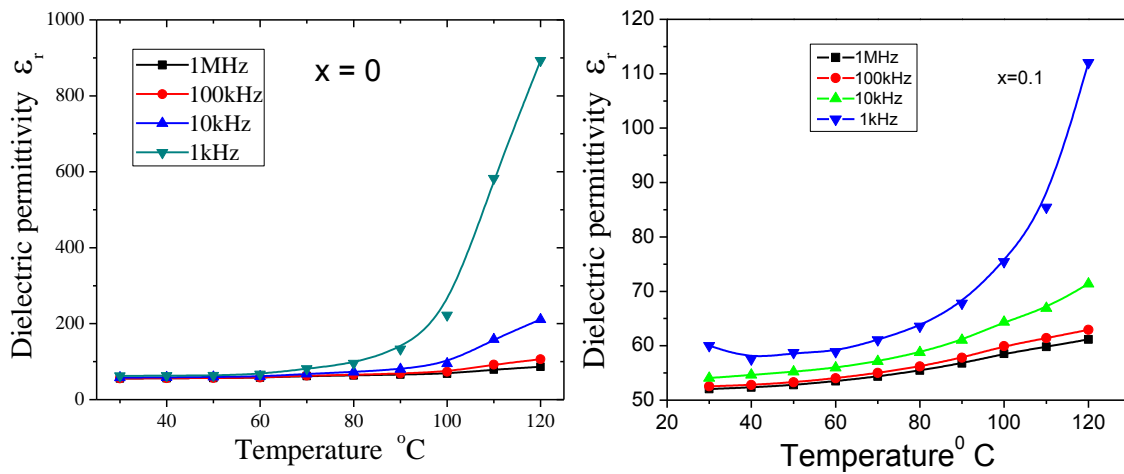


**Fig. 14**. Temperature vs. dielectric constant for PVA-BZT and PVA-BSZT(75:25) vol%

## 4.3.2 Frequency dependence of the dielectric permittivity with different temperature

Figure 15 illustrate the frequency dependence of dielectric constant ($\varepsilon'$) at different temperatures (30-120$^0$C) for PVA: BZT (75:25) and PVA: BSZT (75:25). The dielectric constant increases with increasing temperature. From the plots, it is clear that the permittivity decreases monotonically with increasing frequency and attains a constant value at higher frequencies. Similar behavior has also been observed in other materials. This is because, for polar materials, the initial value of the dielectric permittivity is high, but as the frequency of the field is raised the value begins to drop, which could be because the dipoles are not able to follow the field variation at higher frequencies, as well as polarization effects. At higher frequencies, the periodic reversal of the electric field

occurs so fast that there is no excess ion diffusion in the direction of the field. Hence, the dielectric permittivity ($\varepsilon'$) decreases with increasing frequency in all of the samples.
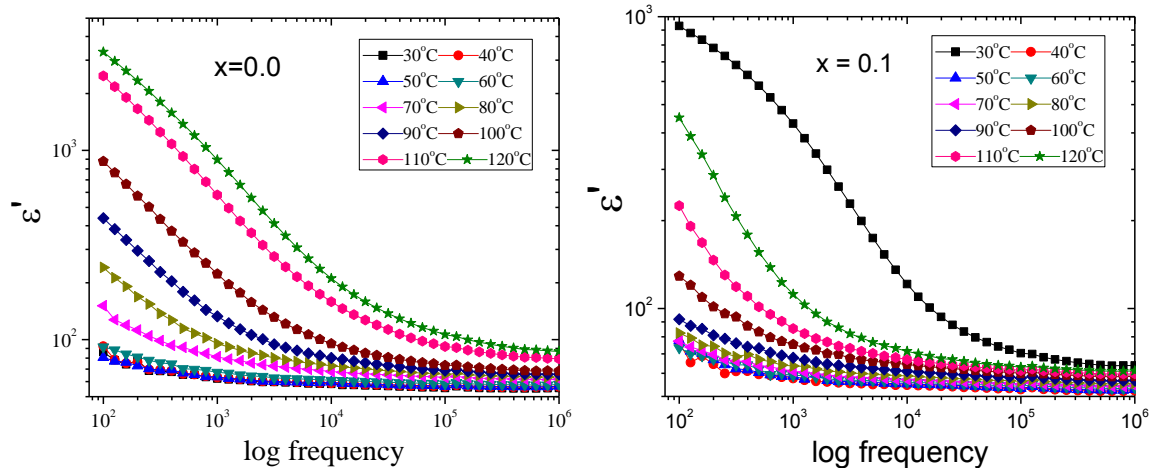


**Fig .15**. Frequency vs. dielectric permittivity for PVA-BZT and PVA-BSZT(75:25) vol%

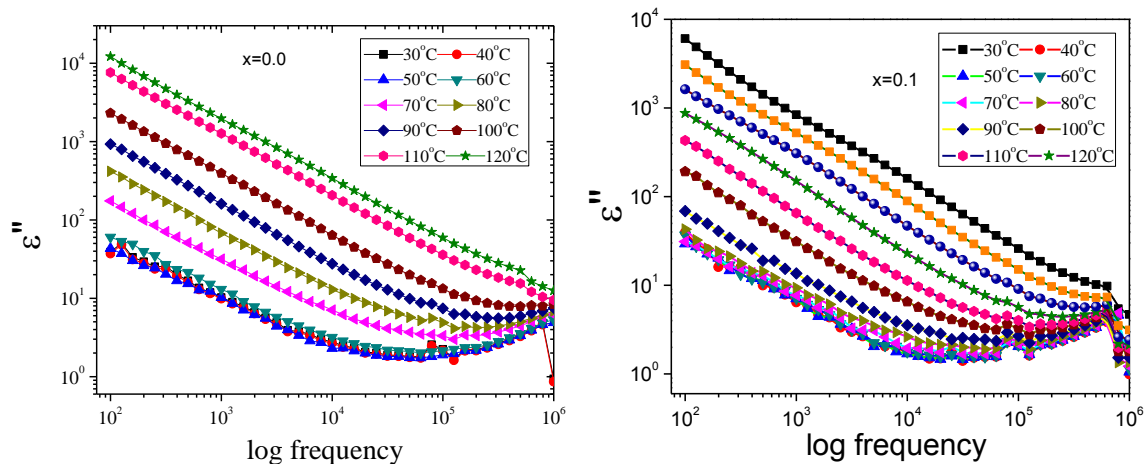## 4.3.3 Frequency dependence of the dielectric loss with different temperatures



**Fig.16** frequency vs. dielectric loss for PVA-BZT and PVA-BSZT(75:25) vol%

Figure 16 shows the variation of $\varepsilon''$ with frequency at different temperatures. At low frequencies and high temperatures $\varepsilon''$ of prepared polymer composite ferroelectric material has very high value which decreases with increase in frequency for up to a certain frequency value, and then again rise at much higher frequency.

### 4.3.4 Frequency dependence of loss tangent

The loss tangent (tan δ) is the ratio of the loss factor to the relative permittivity, and is a measure of the ratio of the electric energy lost to the energy stored in a periodic field. Figure 17 shows the variation of dielectric loss with frequency at different temperatures. From the plots it is clear that tan δ slightly increases with frequency at a particular temperature. The higher dielectric loss that occurs at lower frequency is due to an accumulation of free charge. The polar ionization due to the charge accumulation decreases, leading to a decrease in the value of the dielectric loss.
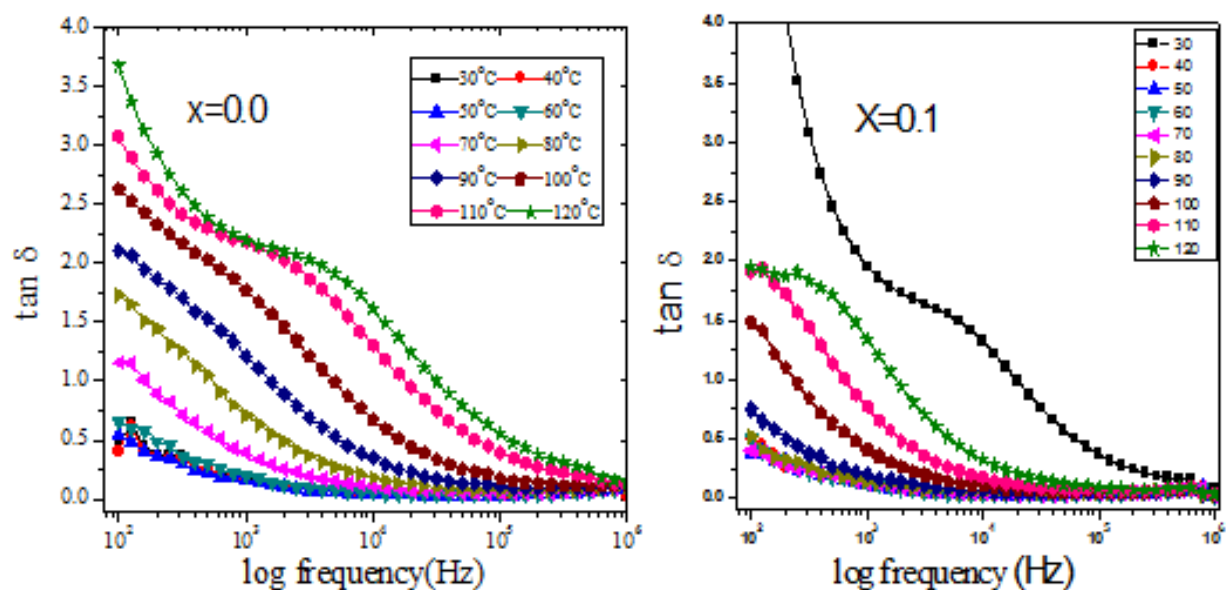


**Fig.17** frequency vs. tan δ for PVA-BZT and PVA-BSZT (75:25) vol%

### 4.3.5 Complex Impedance Spectroscopy

Figure 18 shows that the complex impedance plots (Z" vs Z') of PVA-BZT(75:25) composite and PVA-BSZT(75:25) composite at different temperatures, which corresponding to the properties of bulk material. The large value of imaginary part Z" as compared to real part Z ' of the complex impedance confirm a highly capacitive behaviour of polymer composite ferroelectric material. Normally ceramic samples will show a Poly-dispersive non-Debye type relaxation, due to which the complete semicircle of the complex impedance data will show in a depressed manner (i.e., centre of the semicircle lie below the real axis).
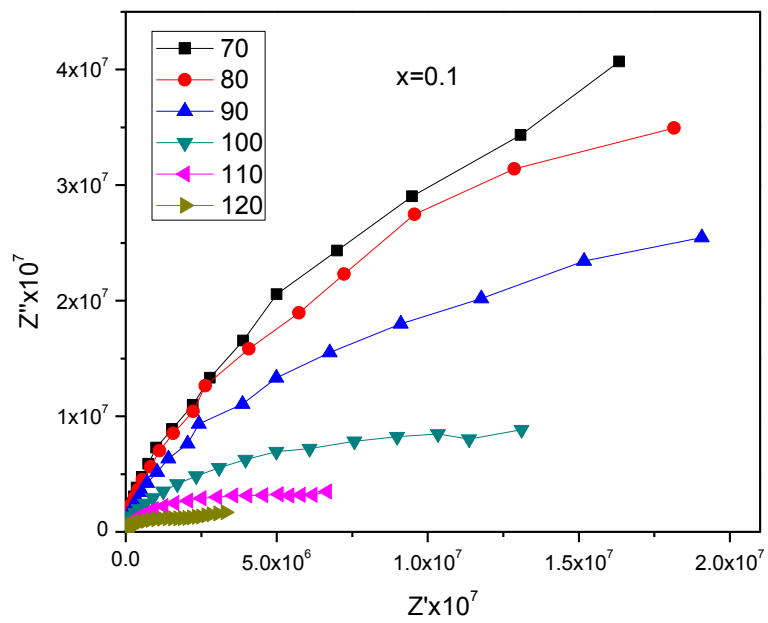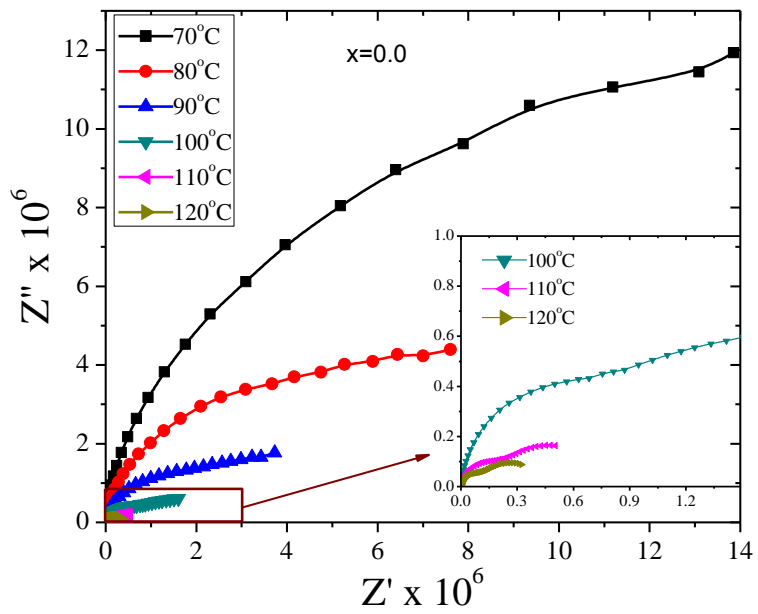
**Fig.18** Z' vs. Z'' for PVA-BZT and PVA-BSZT(75:25) vol%

## 4.3.6 Complex dielectric spectroscopy

The values of $\varepsilon'$ and $\varepsilon''$ obtained from the complex dielectric data, were plotted as complex permittivity ($\varepsilon^*$) spectrum (Cole—Cole plot) (Fig.20). Fig.20 shows a polydispersive relaxation, these Argand plane plots are close to circular arcs with end points on the axis of real and a centre below this axis. In general, the frequency-dependent behavior of $\varepsilon'$ and $\varepsilon''$ of high dielectric permittivity can be well described by the simple Cole–Cole relaxation equation, which ignores the effect of the electrical conduction :

$$\varepsilon* = \ \varepsilon' - j\varepsilon'',$$

$$\varepsilon* = \ \varepsilon_\infty + \frac{\varepsilon_s - \varepsilon_\infty}{1+(j\omega\tau)^{1-\alpha}},$$

where $\varepsilon_s$ and $\varepsilon_\infty$ are respectively, the static and high frequency limits of dielectric permittivity, $\tau$ is the most probable relaxation time and $\alpha$ is the Cole–Cole parameter with values between 0 and 1. For an ideal Debye relaxation, $\alpha = 0$. If $\alpha > 0$, it implies that the relaxation has a distribution of relaxation times, leading to a broader peak shape than a Debye peak. However, when the electrical conductivity is dominated at the low frequency range a contribution term by electrical conduction is generally added to the relaxation equation.
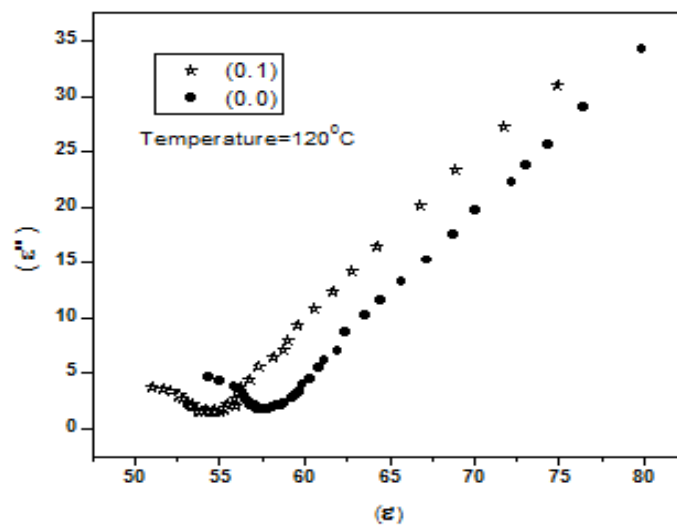


**Fig. 19.** Complex permittivity plot for PVA-BZT and PVA-BSZT(75:25) vol%

# CHAPTER- 5

# CONCLUSION

The ferroelectric material with general formula $Ba_{1-x}Sr_xZr_{0.1}Ti_{0.9}O_3$ (x=0.0,0.1,0.2,0.3) is prepared by conventional solid state reaction method .The X-ray diffraction patterns for all Sr contents single phase BZT compound has been observed without the presence of any impurity peaks with tetragonal structure. The BZT- PVA composite is prepared with different in different volume percentage. The different BSZT-PVA polymer composite is formed with 25 vol %. SEM micrographs shows that the BSZT particle distribution is homogenous with no porous in the PVA matrix. The dielectric study shows that the frequency and temperature dependence dielectric constant and loss. The reason for high dielectric constant in high temperature as well as low frequency is the free polarization of the ceramic materials in the PVA matrix and high dielectric loss is due to the accumulation of free charges. Impedance study shows the Poly-dispersive non-Debye type relaxation, and decrease in grain and grain boundary resistance with increasing temperature.

# REFERENCE

1.   P.Thomas et al,composites Science and Technology 70 (2010) 539

2.   S.U. Adikary et al, composite science and Technology 62 (2002) 2161

3.   Y. Rao, J. Yue, C.P. Wong, Proc. 51st IEEE Conf. Electronic Component Technology, 5th May-6th June, 2001, p. 1408.

4.   C.K. Chiang, R. Popielarz, Ferroelectrics 275 (2002) 1.

5.   L. Ramajo, M. Reboredo, M. Castro, Composites Part A 36 (2005) 1267.

6.   M.K. Temgire et al, Radiation Physics and Chemistry 71 (2004) 1039

7.   Radiation Physics and Chemistry 71 (2004) 1039

8.   Introduction to Solid state Physics by Charles kittle

9.   Introduction to Solid state Physics by Puri and Babber

10.  R.N.P.Choudry et al,physica B 393(2007) 24

11.  R.J.Sengwa et al,eXPRESS polymer letters vol.4,No.9(2010)559

12.  M.Hema et al, journal of Non-Crystalline Solids 355 (2009) 84-90

13.  V.M.Mohan et al,J Polym Res (2010) 17:143

14.  H.C pant et al,Acta Materialia 54 (2006) 3163

15.  Arup Choudhry,Materials Chemistry and Physics 121 (2010) 280

16.  Seung-Hoon Choi et al, Materials Letters 61 (2007) 2478

17.  Gulfam Nasar et al ,J Pak Mater Soc 2009 3 (2)

18.  Izlina Supa et al, Malaysia Polymer International Conference   (MPIC 2009)

19.  M. Sivakumar et al, Materials Chemistry and Physics 97 (2006) 330

20.  T.G. Abdel-Malik et al, Journal of Applied Sciences Research, 4(3): 331, 2008

21.  M.E. Ferna´ ndez et al, Microelectronics Journal 39 (2008) 1344

22.  Tareev B (1979) physics of dielectric materials, MIR publication, Moscow.

23.  Pillai   PKC,   Khurana   P,Trilateral   A(1986)   mater   sci   Lett 5:629.doi:10,1007/BFOI731531